# Triangular $\sqrt{7}$ and quadrilateral $\sqrt{5}$ subdivision schemes: Regular case

Charles K. Chui [a,b,1], Qingtang Jiang [a,*,2], Rokhaya N. Ndao [a]

[a] *Department of Mathematics and Computer Science, University of Missouri–St. Louis, St. Louis, MO 63121, USA*
[b] *Department of Statistics, Stanford University, Stanford, CA 94305, USA*

## Abstract

This paper is devoted to the study of triangular $\sqrt{7}$ and quadrilateral $\sqrt{5}$ surface subdivisions. Both approximation and interpolatory subdivision schemes are considered, with illustrative examples of both scalar-valued and matrix-valued $\sqrt{7}$ and $\sqrt{5}$ subdivision masks that satisfy the sum rule of sufficiently high orders. In particular, "optimal" Sobolev smoothness is determined and Hölder smoothness estimates are presented.

© 2007 Elsevier Inc. All rights reserved.

*Keywords:* Triangular $\sqrt{7}$-subdivisions; Quadrilateral $\sqrt{5}$-subdivisions; Interpolatory schemes; Refinable function vectors; Sum rule orders; Vector subdivisions; Matrix-valued templates; Sobolev smoothness classes; Hölder smoothness estimates

## 1. Introduction

Subdivision algorithms provide the most efficient mathematical tools for parametric curve and surface modeling, rendering, and editing, in Computer Graphics. To generate a smooth surface, a subdivision algorithm is applied to generate a nested sequence of finer meshes that eventually converges to a (smooth) limiting surface, starting from an initial choice of (triangular or quadrilateral) mesh with arbitrary topologies, provided that certain conditions are satisfied. If all the vertices of a coarser mesh (i.e. the mesh before the next iteration step is carried out) are among the vertices of the finer mesh (i.e. the mesh obtained after the next iteration step has been completed), then the subdivision scheme is called an *interpolatory subdivision scheme*. Otherwise, it is called an *approximation subdivision scheme*.

This iterative process is governed by two sets of rules, namely: the *topological rule* that dictates the insertion of new vertices and the connection of them with edges, and the *local averaging rule* for computing the positions in the 3-dimensional space $\mathbb{R}^3$ of the new vertices (and perhaps the new positions of the old ones as well) in terms of certain

---

* Corresponding author. Fax: +1 314 516 5400.

*E-mail address:* jiangq@umsl.edu (Q. Jiang).

[1] Research supported by ARO Grant #W911NF-04-1-0298 and DARPA/NGA Grant #HM1582-05-2-2003.

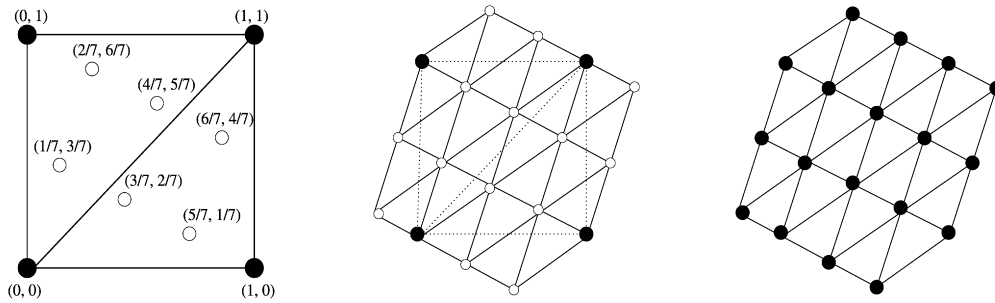[2] Research supported by UMSL Research Awards 02/03, and by UM Research Board 10/05.

Fig. 1. $\sqrt{7}$-Subdivision topological rule.

weighted averages of the (old) vertices within certain neighborhood. For regular vertices (i.e. those with valence 6 for triangular subdivisions, and valence 4 for quadrilateral subdivisions), the rule of the iterative process is described and represented in the plane, called the "parametric domain," by a set of triangles or quadrilaterals of regular shapes along with a set of subdivision templates, usually derived from some refinement (or two-scale) relation of the form:

$$\phi(\mathbf{x}) = \sum_{\mathbf{k} \in \mathbb{Z}^2} p_{\mathbf{k}} \phi(A\mathbf{x} - \mathbf{k}), \quad \mathbf{x} \in \mathbb{R}^2. \tag{1.1}$$

Here, $\phi(\mathbf{x})$ is called a refinable (or two-scale) function with dilation matrix $A$, and the finite sequence $\{p_{\mathbf{k}}\}$ is called its corresponding refinement (or two-scale) sequence. The refinable function $\phi$ is also called the "basis function" of the subdivision scheme, and its corresponding refinement sequence $\{p_{\mathbf{k}}\}$ is commonly called a "subdivision mask."

The choice of the dilation matrix $A$ depends on the topological rule of the subdivision scheme of interest. In this paper, we will give two sets of examples of the matrix $A$ for each of the triangular $\sqrt{7}$ and quadrilateral $\sqrt{5}$ topological rules, construct various subdivision masks, determine their sum rule orders, and their orders on smoothness.

The most popular topological rule for surface subdivisions is the "1-to-4 split" (or dyadic) rule, which dictates the split of each triangle or rectangle in the parametric domain into four sub-triangles or sub-rectangles, respectively. Most of the well-known surface subdivision schemes, including the Catmull and Clark [1], Loop [20], and butterfly [7] schemes, engage the 1-to-4 split topological rule. For the 1-to-4 split rule, the dilation matrix for the corresponding refinement equation to be selected is simply $2I_2$, both for the triangular and quadrilateral meshes. Other topological rules of recent interest include the $\sqrt{3}$ [15–18,23] and the $\sqrt{2}$ [9,10,19,29,30] topological rules, with dilation matrices given, for example, by $\begin{bmatrix} 2 & -1 \\ 1 & -2 \end{bmatrix}$ and $\begin{bmatrix} 1 & 1 \\ 1 & -1 \end{bmatrix}$, respectively. The $\sqrt{3}$ topological rule is designed for the triangular mesh, while the $\sqrt{2}$ rule for the quadrilateral mesh. In this paper, we will study, in some depth, the so-called $\sqrt{7}$ and $\sqrt{5}$ surface subdivision schemes, studied in [11,22].

The triangular $\sqrt{7}$-subdivision was introduced for potential applications to pyramid algorithm design for human vision modeling and for representing structures of very large carbon molecules Chemistry (see [21,27,32]). Its topological rule is shown graphically in Fig. 1. For the purpose of finding the dilation matrices $A$, let us describe in details how the finer mesh in the parametric domain of entire $x$–$y$ plane is derived from the coarser mesh, described by the triangulation with grid lines $x = i$, $y = j$, $x - y = k$, by applying the $\sqrt{7}$ topological rule transform once. For each vertex $\mathbf{k} \in \mathbb{Z}^2$ of this coarser mesh, we put three points $\mathbf{k} + \frac{1}{7}(3, 2)$, $\mathbf{k} + \frac{1}{7}(5, 1)$, $\mathbf{k} + \frac{1}{7}(6, 4)$ inside the triangle with vertices $\mathbf{k}, \mathbf{k} + (1, 0)$ and $\mathbf{k} + (1, 1)$ and three points $\mathbf{k} + \frac{1}{7}(1, 3)$, $\mathbf{k} + \frac{1}{7}(4, 5)$, $\mathbf{k} + \frac{1}{7}(2, 6)$ inside the triangle with vertices $\mathbf{k}, \mathbf{k} + (1, 1)$ and $\mathbf{k} + (0, 1)$. These points so chosen will be called new vertices (see the figure on the left of Fig. 1, where $\mathbf{k} = (0, 0)$), while the vertices of the coarser mesh will be called old vertices. The following two steps describe how the finer mesh is obtained as a result of applying the $\sqrt{7}$ topological rule once. The first step is to connect each of the new vertices with the closest old vertex as well as five closest new vertices, which lie in three different triangles. This yields the new edges given by the lines with slopes $\frac{2}{3}, 3, -\frac{1}{2}$ (see the figure in the middle of Fig. 1, where the coarser mesh is represented by the dotted lines). The second step is to remove the edges of the coarser mesh as shown in the figure on the right of Fig. 1. See also the figure on the left of Fig. 2, where the coarser mesh is represented by the dotted lines and the finer mesh by the solid lines. Another formulation of the finer mesh is obtained simply by reflection across the line $x = y$ of the finer mesh shown in the figure on the left. In other words, this other formulation of the finer mesh consists of grid lines with slopes $\frac{3}{2}, \frac{1}{3}, -2$ as shown in the figure on the right of Fig. 2, where again, dotted straight lines are used for the coarser mesh and solid straight lines for the finer mesh.
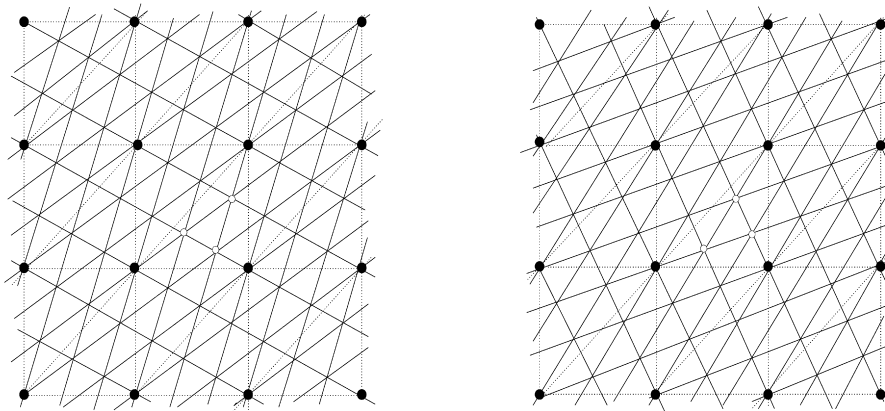
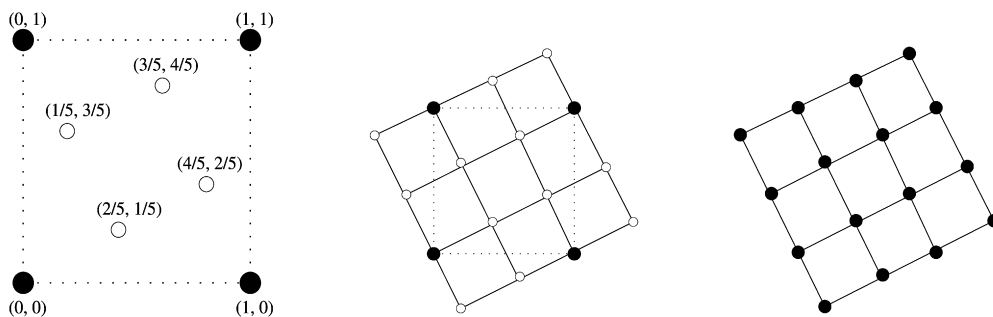Fig. 2. Two types of finer meshes in parametric domain after $\sqrt{7}$-subdivision.



Fig. 3. $\sqrt{5}$-subdivision topological rule.

In [22], by applying composite operations, $\sqrt{7}$-subdivision schemes with high smooth orders were constructed. However, as also mentioned in [22], the composite approach cannot lead to interpolatory schemes even to achieve $C^1$ smoothness. In this paper, we will outline a procedure, with demonstrative examples, for constructing both interpolatory and approximation $\sqrt{7}$-subdivision schemes to achieve desirable order of smoothness.

To describe the quadrilateral $\sqrt{5}$-subdivision, let us consider the rectangular grid consisting of the horizontal lines $x = i$ and vertical lines $y = j$, $i, j \in \mathbb{Z}$, as the coarser mesh. First, for each $\mathbf{k} \in \mathbb{Z}^2$, select four points $\mathbf{k} + \frac{1}{5}(2, 1)$, $\mathbf{k} + \frac{1}{5}(4, 2), \mathbf{k} + \frac{1}{5}(3, 4), \mathbf{k} + \frac{1}{5}(1, 3)$ (to be called new vertices) within the square with vertices $\mathbf{k}, \mathbf{k} + (1, 0), \mathbf{k} + (1, 1)$ and $\mathbf{k} + (0, 1)$. See the figure on the left of Fig. 3 for $\mathbf{k} = (0, 0)$. Then connect each of the new vertices with the closest vertex of the coarser mesh as well as three closest new vertices, that lie in different rectangles, to yield the new edges, as given by the lines with slopes $\frac{1}{2}$, $-2$ (see the figure in the middle of Fig. 3, where the coarser mesh is represented by the dotted lines). Finally, the finer mesh, obtained after applying the $\sqrt{5}$ topological rule once, is achieved by removing the coarser mesh as shown in the figure on the right of Fig. 3. For the purpose of finding the dilation matrices $A$, we also show the mesh in the entire $x$–$y$ plane, on the left of Fig. 4, where the coarser mesh consists of the horizontal and vertical dotted lines, and the finer mesh is represented by the solid lines. Similarly, another formulation of the finer mesh, as shown on the right of Fig. 4, is obtained simply by reflection across the line $x = y$ of the finer mesh in the figure on the right. The $\sqrt{5}$ rule was first proposed in [28] as a hierarchical sampling scheme over a regular mesh because of the unique property that the five vertices in each group that corresponds to a quadrilateral of the coarser mesh, consisting of one old vertex and four new vertices, have different $x$ and $y$ coordinates. A $C^1$ approximation $\sqrt{5}$-subdivision scheme was constructed in [11]. In our present paper, we will construct both interpolatory and approximation $\sqrt{5}$-subdivision schemes to achieve both $C^1$ and $C^2$ smoothness.

In the construction of any interpolatory subdivision scheme, we must face the same dilemma as in the construction of 1-to-4 split interpolatory subdivision schemes, in that subdivision templates with undesirably large size are needed to achieve subdivision surfaces of any higher order of smoothness. Such subdivision templates are in general too large to be useful in practice, particularly when they have to be adjusted near extraordinary vertices. For this reason, vector
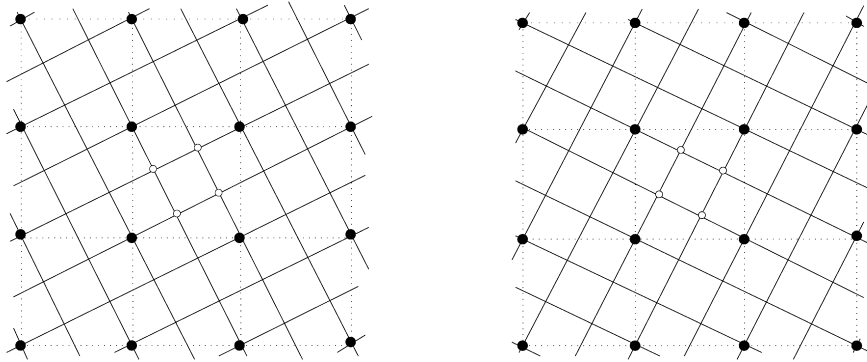
Fig. 4. Two types of finer meshes in parametric domain after $\sqrt{5}$-subdivision.

subdivisions for surface design were recently studied in our work [2–6] to provide subdivision templates of minimal size. Analogous to scalar subdivisions, a vector subdivision scheme for regular vertices is also derived from some refinement (or two-scale) equation

$$\Phi(\mathbf{x}) = \sum_{\mathbf{k} \in \mathbb{Z}^2} P_{\mathbf{k}} \Phi(A\mathbf{x} - \mathbf{k}), \quad \mathbf{x} \in \mathbb{R}^2, \tag{1.2}$$

but with matrix-valued mask $\{P_{\mathbf{k}}\}$, where $\Phi = [\phi_0, \ldots, \phi_{r-1}]^T$ is called a refinable (or two-scale) function vector. Corresponding to the refinement equation (1.2), the local averaging rule, from which the subdivision templates (with matrix-valued weights) can be written down immediately, is given by

$$\mathbf{v}_{\mathbf{k}}^{m+1} = \sum_{\mathbf{j}} \mathbf{v}_{\mathbf{j}}^m P_{\mathbf{k} - A\mathbf{j}}, \quad m = 0, 1, \ldots, \tag{1.3}$$

where

$$\mathbf{v}_{\mathbf{k}}^m =: \left[ v_{\mathbf{k}}^m, s_{\mathbf{k},1}^m, \ldots, s_{\mathbf{k},r-1}^m \right] \tag{1.4}$$

are "row-vectors" with $r$ components of points $v_{\mathbf{k}}^m, s_{\mathbf{k},i}^m, i = 1, \ldots, r-1$, in $\mathbb{R}^3$. Here, the first components $v_{\mathbf{k}}^m$ are the vertices of the triangular or (non-planar) quadrilateral meshes for the $m$th iteration, with $v_{\mathbf{k}}^0$ being the control vertices of the surface subdivision. We call the initial (full) row vectors $\mathbf{v}_{\mathbf{k}}^0$ "control vectors," and the other components $s_{\mathbf{k},1}^0, \ldots, s_{\mathbf{k},n-1}^0$ of $\mathbf{v}_{\mathbf{k}}^0$, "shape-control parameters." In [5], we have shown that under certain conditions, including the so-called "generalized partition of unity," the vertices $v_{\mathbf{k}}^m$, for sufficiently large values of $m$, provide an accurate discrete approximation of the target subdivision surface, given by the series representation:

$$F(\mathbf{x}) = \sum_{\mathbf{k}} v_{\mathbf{k}}^0 \phi_0(\mathbf{x} - \mathbf{k}) + \sum_{\mathbf{k}} \left( s_{\mathbf{k},1}^0 \phi_1(\mathbf{x} - \mathbf{k}) + \cdots + s_{\mathbf{k},n-1}^0 \phi_{n-1}(\mathbf{x} - \mathbf{k}) \right).$$

We have demonstrated in [5] that the shape-control parameters $s_{\mathbf{k},1}^0, \ldots, s_{\mathbf{k},n-1}^0$, could be used to control the shape of the subdivision surface dramatically.

The most natural definition of interpolatory vector subdivisions was studied in [4], where we say that a vector subdivision scheme, with subdivision mask $\{P_{\mathbf{k}}\}$ and dilation matrix $A$, is interpolatory if $v_{A\mathbf{k}}^{m+1} = v_{\mathbf{k}}^m, m = 0, 1, \ldots, \mathbf{k} \in \mathbb{Z}^2$. Here, $v_{A\mathbf{k}}^{m+1}$ and $v_{\mathbf{k}}^{m+1}$ are the first components of $\mathbf{v}_{A\mathbf{k}}^{m+1}$ and $\mathbf{v}_{\mathbf{k}}^{m+1}$, respectively. This definition precisely assures that the control vertices lie on the parametric subdivision surface, as in the scalar-valued setting. The algebraic structure of an interpolatory mask $\{P_{\mathbf{k}}\}$ for the vector-valued setting is given by

$$P_{0,0} = \begin{bmatrix} 1 & * & \cdots & * \\ 0 & * & \cdots & * \\ \vdots & \vdots & \cdots & \vdots \\ 0 & * & \cdots & * \end{bmatrix}, \quad P_{A\mathbf{j}} = \begin{bmatrix} 0 & * & \cdots & * \\ \vdots & \vdots & \cdots & \vdots \\ 0 & * & \cdots & * \end{bmatrix}, \quad \mathbf{j} \in \mathbb{Z}^2 \backslash \{(0,0)\}. \tag{1.5}$$

Observe that when the dimension $r$ is reduced to 1, this property is equivalent to the simple algebraic property

$$p_{A\mathbf{j}} = \delta(\mathbf{j}), \quad \mathbf{j} \in \mathbb{Z}^2, \tag{1.6}$$

of an interpolatory mask $\{p_{\mathbf{k}}\}$ for the scalar-valued setting.

We have constructed, in [4], illustrative examples of $C^2$ interpolatory vector 1-to-4 split, $\sqrt{3}$ and $\sqrt{2}$ subdivision schemes with matrix-valued templates with "minimum size." In the same paper, we have also constructed $C^2$ interpolatory vector 1-to-4 split, $\sqrt{3}$ and $\sqrt{2}$ subdivision schemes with $C^2$-cubic splines and $C^2$-quartic splines as basis functions, which, as is well known, cannot be achieved in the scalar setting.

One of the main objectives of this present paper is to construct vector interpolatory $\sqrt{7}$ and $\sqrt{5}$ subdivision schemes for regular vertices. As to extraordinary vertices, one could also design certain local averaging rules to achieve $C^1$-continuity in a similar way as the scalar-valued setting studied by [26]. For this purpose, the $C^1$-continuity condition developed in [5] can be used as the design specification. Unfortunately, this is not an easy task for $\sqrt{7}$ and $\sqrt{5}$ subdivisions, and our work in this direction will be published elsewhere. In general, we have extended the $C^k$-continuity conditions of [25,26] from the scalar-valued setting to the general matrix-valued setting in [5].

The rest of this paper is organized as follows. In Section 2, certain necessary preliminary materials on sum rule orders of the subdivision mask and smoothness estimates of the basis functions or function vectors are discussed. Our results on $\sqrt{7}$-subdivision and $\sqrt{5}$-subdivision schemes will be presented in Sections 3 and 4, respectively.

## 2. Preliminaries

Let us first take care of some standard notations. $\mathbb{N}$ will denote the set of positive integers, and $\mathbb{Z}_+$, the set of non-negative integers. An ordered pair $\mu = (\mu_1, \mu_2) \in \mathbb{Z}_+^2$ is called a multi-index. The length of $\mu$ is denoted by $|\mu| := \mu_1 + \mu_2$ and the factorial $\mu!$ of $\mu$, by $\mu! := \mu_1! \mu_2!$. In addition, the partial derivative of a differentiable function $f$ with respect to the $j$th coordinate is denoted by $D_j f$, $j = 1, 2$, and for $\mu = (\mu_1, \mu_2) \in \mathbb{Z}_+^2$, $D^\mu$ denotes the differential operator $D_1^{\mu_1} D_2^{\mu_2}$. For a set $\Omega \subset \mathbb{R}^2$, we introduce the notation

$$[\Omega] := \Omega \cap \mathbb{Z}^2.$$

Next, for $s \geqslant 0$, a function $f$ is said to be in the Sobolev space $W^s(\mathbb{R}^2)$, if its Fourier transform $\hat{f}(\omega)$ satisfies $(1 + |\omega|^2)^{\frac{s}{2}} \hat{f}(\omega) \in L^2(\mathbb{R}^2)$. Let $s_2(f)$ denote its *critical Sobolev exponent* defined by

$$s_2(f) := \sup\{s : f \in W^s(\mathbb{R}^2)\}.$$

For a vector-valued function $F = [f_0, \ldots, f_{r-1}]^T$, we will use the analogous notation

$$s_2(F) := \min\{s_2(f_j) : 0 \leqslant j \leqslant r - 1\}.$$

On the other hand, the critical Hölder exponent is defined as follows. For a function $f \in C(\mathbb{R}^2)$, the $j$th difference in the direction $t \in \mathbb{R}^2$ is denoted by

$$\nabla_t^j f := \nabla_t^1 (\nabla_t^{j-1} f), \qquad \nabla_t^1 f(x) := f(x) - f(x - t), \quad x \in \mathbb{R}^2.$$

Then the $j$th modulus of smoothness is defined by

$$\omega_j(f, h) := \sup_{|t| \leqslant h} \|\nabla_t^j f\|_C, \quad h \geqslant 0.$$

We also use the standard notation Lip$(s)$, $s > 0$, for the generalized (Lipschitz–)Hölder class consisting of all bounded functions $f \in C(\mathbb{R}^2)$ with

$$\omega_j(f, h) \leqslant Ch^s, \quad h > 0,$$

where $C$ is a constant independent of $h$, and $j$ is any fixed integer greater than $s$. We remark that it is a common practice to set $C^s(\mathbb{R}^2) := \text{Lip}(s)$ for non-integer $s > 0$ to extend the definition of the spaces of $k$-times continuously differentiable functions, for positive integers $k$. Then the *critical Hölder exponent of* $f$ is defined by

$$s_\infty(f) := \sup\{s : f \in \text{Lip}(s)\}.$$

Also, analogous to Sobolev exponents for vector-valued functions, the *critical Hölder exponent* of a vector-valued function $F = [f_0, \ldots, f_{r-1}]^T$ is defined by

$$s_\infty(F) := \min\{s_\infty(f_j): 0 \leqslant j \leqslant r-1\}.$$

We remark that by the Sobolev imbedding theorem, we have

$$s_\infty(F) \geqslant s_2(F) - 1.$$

Let $A$ be a $2 \times 2$ dilation matrix in (1.1) or (1.2), and assume that $A$ is similar to a diagonal matrix $\operatorname{diag}(\lambda_1, \lambda_2)$ with $|\lambda_1| = |\lambda_2|$. Set

$$\sigma := (\lambda_1, \lambda_2)$$

and

$$s := |\det A|.$$

Then taking the Fourier transform of both sides of (1.2), we obtain

$$\hat{\Phi}(\omega) = P(A^{-T}\omega)\hat{\Phi}(A^{-T}\omega), \quad \omega \in \mathbb{R}^2, \tag{2.1}$$

where $A^{-T}$ denotes the transpose of $A^{-1}$, and

$$P(\omega) := \frac{1}{s} \sum_{\mathbf{k} \in \mathbb{Z}^2} P_{\mathbf{k}} e^{-i\mathbf{k}\cdot\omega}, \quad \omega \in \mathbb{R}^2, \tag{2.2}$$

is the *symbol* associated with $\{P_{\mathbf{k}}\}$. Here, $P(\omega)$ is an $r \times r$ matrix with trigonometric polynomial entries.

Let $\eta_j + A^T\mathbb{Z}^2$, $j = 0, \ldots, s-1$, be the $s$ distinct elements of $\mathbb{Z}^2/(A^T\mathbb{Z}^2)$ with $\eta_0 = 0$. For the scalar-valued setting with $r = 1$, we say that $P(\omega)$ or $\{P_{\mathbf{k}}\}$ satisfies the *sum rule of order k* if

$$P(0) = 1, \qquad D^\mu P(2\pi A^{-T}\eta_j) = 0, \quad j = 1, \ldots, s-1, \ |\mu| < k. \tag{2.3}$$

For $r > 1$, we say that $P$ satisfies *sum rule of order k* provided there exists a $1 \times r$ function vector $B(\omega)$ with trigonometric polynomial components and $B(0) \neq \mathbf{0}$, such that

$$D^\mu(B(A^T\cdot)P(\cdot))(2\pi A^{-T}\eta_j) = \delta(j)D^\mu B(0), \quad j = 0, \ldots, s-1, \ |\mu| < k. \tag{2.4}$$

By setting

$$\mathbf{y}_\alpha := (-iD)^{\boldsymbol{\alpha}}\mathbf{B}(0), \quad |\boldsymbol{\alpha}| < k, \tag{2.5}$$

it follows that

$$\mathbf{x}^{\mathbf{j}} = \sum_{\mathbf{k}} \left\{ \sum_{\boldsymbol{\alpha} \leqslant \mathbf{j}} \frac{\mathbf{j}!}{\boldsymbol{\alpha}!(\mathbf{j}-\boldsymbol{\alpha})!} \mathbf{k}^{\mathbf{j}-\boldsymbol{\alpha}}\mathbf{y}_\alpha \right\} \Phi(\mathbf{x}-\mathbf{k}), \quad \mathbf{x} \in \mathbb{R}^2, \ \mathbf{j} \in \mathbb{Z}_+^2, \ |\mathbf{j}| < k. \tag{2.6}$$

This is an explicit local polynomial preservation formula in terms integer translates of $\Phi$ (see the survey paper [13] and the references therein for more details).

Without loss of generality, assume that the support of the subdivision mask $\{P_{\mathbf{k}}\}$ is in $[-N, N]^2$, i.e., $P_{\mathbf{k}} = 0$, $\mathbf{k} \notin [-N, N]^2$, for some $N > 0$. Let

$$\Omega := \left\{ \sum_{j=1}^\infty A^{-j}x_j: x_j \in [-N, N]^2, \ \forall j \in \mathbb{N} \right\}, \tag{2.7}$$

and consider the matrix

$$T_P = [B_{A\mathbf{k}-\mathbf{j}}]_{\mathbf{k},\mathbf{j}\in[\Omega]}, \tag{2.8}$$

where

$$B_{\mathbf{j}} = \frac{1}{s} \sum_{\mathbf{k}} P_{\mathbf{k}-\mathbf{j}} \otimes \overline{P}_{\mathbf{k}},$$

and $\otimes$ denotes the Kronecker product of $A$ and $B$, namely $A \otimes B = [a_{ij}B]$.

In the following, assume that $P(\omega)$ satisfies the sum rule of order $k$ and that the matrix $P(0)$ is similar to a diagonal matrix $\mathrm{diag}(1, \lambda_2, \ldots, \lambda_r)$ with $|\lambda_j| < 1$, $j = 2, \ldots, r$. Set

$$S_k := \mathrm{spec}(T_P) \backslash \bar{S}_k, \tag{2.9}$$

where

$$\bar{S}_k := \left\{ \sigma^{-\alpha} \overline{\lambda_j}, \overline{\sigma^{-\alpha}} \lambda_j, \sigma^{-\beta} \colon \alpha, \beta \in \mathbb{Z}_+^2, \ |\alpha| < k, \ |\beta| < 2k, \ 2 \leqslant j \leqslant r \right\};$$

and

$$\rho_0 = \max \left\{ |\lambda| \colon \lambda \in S_k \right\}.$$

It was shown in [14] that

$$s_2(\Phi) \geqslant -\log_s \rho_0, \tag{2.10}$$

and that if $\Phi$ is $L^2$-stable, then we have

$$s_2(\Phi) = -\log_s \rho_0. \tag{2.11}$$

We will use the formula in (2.10) to compute the Sobolev smoothness estimates of refinable function/vectors $\Phi$.

Next, let us consider the Hölder smoothness estimates $v_\infty(\Phi)$ of refinable function/vectors $\Phi$. For a finite set $\mathcal{A}$ of operators acting on a fixed finite-dimensional space $V$, the *joint spectral radius* $\rho_\infty(\mathcal{A})$ of $\mathcal{A}$ is defined by

$$\rho_\infty(\mathcal{A}) := \lim_{l \to \infty} \left\| \mathcal{A}^l \right\|_\infty^{1/l},$$

where

$$\left\| \mathcal{A}^l \right\|_\infty := \max \left\{ \|A_1 \cdots A_l\| \colon A_n \in \mathcal{A}, \ 1 \leqslant n \leqslant l \right\}.$$

Here, the operator norm $\| \cdot \|$ is induced by the norm on $V$ and the value of $\rho_\infty(\mathcal{A})$ does not depend on the choice of the latter. The interested reader is referred to [24,33] on the computational aspect of joint spectral radii.

Let $\gamma_j + A\mathbb{Z}^2$, $j = 0, \ldots, s-1$, be the $s$ distinct elements of $\mathbb{Z}^2/(A\mathbb{Z}^2)$ with $\gamma_0 = 0$. Set $\Gamma := \{\gamma_j, \ j = 0, 1, \ldots, s-1\}$. Let $P = \{P_{\mathbf{k}}\}_{\mathbf{k} \in [-N,N]^2}$ be a subdivision mask satisfying the sum rule of order $k$, namely, (2.4) for some $B(\omega) = \sum_{\mathbf{k} \in [-N,N]^2} B_{\mathbf{k}} e^{-i\mathbf{k}\omega}$. For $\gamma \in \Gamma$, define the operators $A_{P,\gamma}$, on $\ell_0(\mathbb{Z}^2)^{r \times 1}$ by

$$(A_{P,\gamma} v)_\alpha = \sum_{\beta \in \mathbb{Z}^2} P_{\gamma + A\alpha - \beta} v_\beta, \quad \alpha \in \mathbb{Z}^2, \ v \in \ell_0(\mathbb{Z}^2)^{r \times 1}. \tag{2.12}$$

In the following, we use the notation

$$\Omega_1 := \left\{ \sum_{j=1}^\infty A^{-j} x_j \colon x_j \in [-N, N]^2 - \Gamma, \ \forall j \in \mathbb{N} \right\}. \tag{2.13}$$

Let $V_k$ be the subspace of $\ell(\mathbb{Z}^2)^{r \times 1}$ consisting of $v$ with support in $[\Omega_1]$ that satisfy

$$D^\nu \big( B(\omega) v(\omega) \big) \big|_{\omega = 0} = 0, \quad |\nu| < k, \tag{2.14}$$

where $v(\omega) := \sum_{\alpha \in [\Omega_1]} v_\alpha e^{-i\alpha\omega}$. Note that $V_k$ is a finite-dimensional space and is invariant under the operators $A_{P,\gamma}, \gamma \in \Gamma$. Denote by $\rho_k$ the joint spectral radius of the family $\mathcal{A}_k := \{A_{P,\gamma}|_{V_k}, \ \gamma \in \Gamma\}$. Then, we have

$$s_\infty(\Phi) \geqslant -2 \log_s \rho_k. \tag{2.15}$$

In practice, it is difficult to find the joint spectral radius $\rho_k$ in general. Instead, we consider sequences of lower and upper estimates, namely:

$$\underline{\rho}_k^l := \max \left\{ \rho(A_1 \cdots A_l)^{1/l} \colon A_n \in \mathcal{A}_k, \ 1 \leqslant n \leqslant l \right\}$$
$$\leqslant \rho_k \leqslant \overline{\rho}_k^l := \max \left\{ \|A_1 \cdots A_l\|_2^{1/l} \colon A_n \in \mathcal{A}_k, \ 1 \leqslant n \leqslant l \right\}, \tag{2.16}$$

where $\| \cdot \|_2$ denotes the spectral norm for matrix operators. Set

$$\bar{s}_\infty^l(\Phi) := -2\log_s \underline{\rho}_k^l, \qquad \underline{s}_\infty^l(\Phi) := -2\log_s \overline{\rho}_k^l. \tag{2.17}$$

We will use $\bar{s}^l_\infty(\Phi)$ and $\underline{s}^l_\infty(\Phi)$ in (2.17) to give Hölder smoothness estimates of $\Phi$. In practice, depending on the support of $\{P_\mathbf{k}\}_{\mathbf{k}\in[-N,N]^2}$, one could choose some subset of $V_k$ which is invariant under $A_{P,\gamma}$, $\gamma \in \Gamma$, for an appropriate subset of $[\Omega_1]$. In the scalar-valued setting, if $P(\omega) \geqslant 0$, then $s_\infty(\phi) = \underline{s}^1_\infty(\phi)$, see [8,12,31].

In the next two sections, we will construct various approximation and interpolatory $\sqrt{7}$ and $\sqrt{5}$ subdivision schemes, for both the scalar and vector settings. Following [4], the general procedure is outlined as follows:

(i) Formulate a subdivision mask $\{P_\mathbf{k}\}$ of an acceptable size that satisfies certain symmetry properties, as governed by the need of symmetry for the subdivision templates. Start with zero values for most of the weights, but allow non-zero values gradually, to provide sufficient freedom to accommodate the requirements of the desired sum rule order and the order of smoothness.

(ii) Formulate a set of linear equations with scalar or matrix entries that have not yet been determined as unknowns, by imposing the requirement of the desired sum rule orders (2.3) or (2.4). In addition, to construct interpolatory schemes, the interpolatory conditions (1.6) or (1.5) is imposed as constraints on the unknowns.

(iii) The general solution of the equations is formulated in terms of some free parameters.

(iv) Finally, the free parameters are to be adjusted by applying the algorithm/software in [14]/[15] to achieve the "optimal" Sobolev smoothness, namely by maximizing $-\log_s \rho_0$.

In addition to (iv), we may also need the Hölder smoothness estimates, determined by applying (2.17), to ensure that the subdivision schemes are $C^1$ or $C^2$ schemes.

## 3. $\sqrt{7}$-Subdivision schemes

First we need to find a dilation matrix $A$ for the $\sqrt{7}$-subdivision. Such dilation matrices should have integer entries, and as a convenient guideline, their inverses should map the coarse mesh onto one of the finer meshes in Fig. 2. There are many choices for the matrix $A$ that satisfy the above-mentioned properties, namely:

$$\pm\begin{bmatrix} 3 & -1 \\ 1 & 2 \end{bmatrix}, \quad \pm\begin{bmatrix} 2 & -3 \\ 3 & -1 \end{bmatrix}, \quad \pm\begin{bmatrix} 1 & 2 \\ -2 & 3 \end{bmatrix}, \quad \pm\begin{bmatrix} 3 & -2 \\ 2 & 1 \end{bmatrix}, \quad \pm\begin{bmatrix} 2 & 1 \\ -1 & 3 \end{bmatrix}, \quad \pm\begin{bmatrix} 1 & -3 \\ 3 & -2 \end{bmatrix}, \tag{3.1}$$

and

$$\pm\begin{bmatrix} 1 & 2 \\ 3 & -1 \end{bmatrix}, \quad \pm\begin{bmatrix} 3 & -1 \\ 2 & -3 \end{bmatrix}, \quad \pm\begin{bmatrix} -2 & 3 \\ 1 & 2 \end{bmatrix}, \quad \pm\begin{bmatrix} 2 & 1 \\ 3 & -2 \end{bmatrix}, \quad \pm\begin{bmatrix} -1 & 3 \\ 2 & 1 \end{bmatrix}, \quad \pm\begin{bmatrix} 3 & -2 \\ 1 & -3 \end{bmatrix}. \tag{3.2}$$

We remark that the dilation matrix $\begin{bmatrix} 2 & 1 \\ -1 & 3 \end{bmatrix}$, from the list in (3.1), was used in the paper [22]. The dilation matrices in the second list (3.2), satisfy $A^2 = 7I_2$. In this paper we choose

$$M := \begin{bmatrix} 1 & 2 \\ 3 & -1 \end{bmatrix} \tag{3.3}$$

from the second list (3.2), and consider the corresponding finer mesh as shown on the left of Fig. 2. For this dilation matrix $M$, the choice of

$$\eta_0 = (0,0), \quad \eta_1 = (1,0), \quad \eta_2 = (0,1), \quad \eta_3 = (-1,0),$$
$$\eta_4 = (0,-1), \quad \eta_5 = (1,-1), \quad \eta_6 = (-1,1), \tag{3.4}$$

results in 7 distinct elements $\eta_j + M^T\mathbb{Z}^2$, $j = 0, \ldots, 6$, of $\mathbb{Z}^2/(M^T\mathbb{Z}^2)$.

In the following two subsections, we will discuss scalar and vector $\sqrt{7}$-subdivision schemes separately.

### 3.1. Scalar $\sqrt{7}$-subdivision schemes

We will use the general templates with restricted size, as shown in Fig. 5, for deriving the local averaging rules that meet certain requirements on sum rule orders and smoothness conditions. Observe that for this study of scalar subdivisions, the values $x = 1$ and $y = 0$ in the template on the left of Fig. 5 correspond to interpolating subdivision schemes. The subdivision mask $\{p_\mathbf{k}\}$ associated with the templates in Fig. 5 is given by the matrix in (3.5), whose
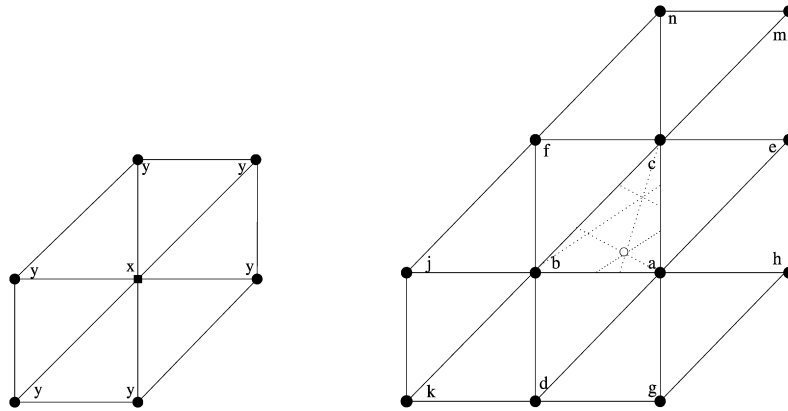
Fig. 5. Templates for scalar $\sqrt{7}$-subdivision schemes.

$(k_1, k_2)$-entry will be denoted by $p_{k_2-6,-(k_1-6)}$, to match the notation in (1.1), where the dilation matrix $A$ is given by the matrix $M$ in (3.3).

$$
\begin{bmatrix}
0 & 0 & 0 & 0 & 0 & 0 & n & j & m & 0 & 0 \\
0 & 0 & 0 & 0 & 0 & k & h & g & f & k & n \\
0 & 0 & 0 & m & f & e & y & d & e & h & j \\
0 & 0 & j & g & d & c & b & c & y & g & m \\
0 & n & h & y & b & a & a & b & d & f & 0 \\
0 & k & e & c & a & \mathbf{x} & a & c & e & k & 0 \\
0 & f & d & b & a & a & b & y & h & n & 0 \\
m & g & y & c & b & c & d & g & j & 0 & 0 \\
j & h & e & d & y & e & f & m & 0 & 0 & 0 \\
n & k & f & g & h & k & 0 & 0 & 0 & 0 & 0 \\
0 & 0 & m & j & n & 0 & 0 & 0 & 0 & 0 & 0
\end{bmatrix}. \tag{3.5}
$$

### 3.1.1. Approximation $\sqrt{7}$-subdivision scalar templates

First we consider subdivision schemes with reasonable small template sizes, namely: $g = h = j = k = m = n = 0$. Let $\{p_{\mathbf{k}}\}$ be the corresponding mask and $p(\omega) = \frac{1}{7}\sum_{\mathbf{k}} p_{\mathbf{k}} e^{-i\mathbf{k}\omega}$. We then eliminate some of the parameters $a, b, c, d, e, f, x, y$ by considering the mask $\{p_{\mathbf{k}}\}$ with sum rule of order 3 and particularly the linear system governed by

$$
p(0) = 1, \qquad D^{\mu} p\left(2\pi M^{-T} \eta_j\right) = 0, \quad j = 1, \ldots, 6, \ |\mu| < 3, \tag{3.6}
$$

with $\eta_j$ given by (3.4). Then solution of this linear system (3.6) yields

$$
\begin{aligned}
x &= 31/49 - 3f, \quad y = 3/49 + f/2, \quad a = 24/49 - f, \\
b &= 12/49 - f, \quad c = 9/49 - f, \quad d = 3/49 + f, \quad e = 1/49 + f.
\end{aligned} \tag{3.7}
$$

Hence, we have a family of subdivision masks of sum rule order 3.

Following procedure (iv) (to maximize $-\log_7 \rho_0$), we can obtain, for $f = -0.003703$, the refinable function with the highest order of Sobolev smoothness $\phi \in W^{2.786639}$. The plot of Sobolev smoothness exponents of $\phi$ against the parameter $f$ is shown on the left of Fig. 6, with the zoom-in to the maximum near 0 on the right. The following two particular values of $f$ that are close to the maximum of the Sobolev exponents are of particular interesting to us. One is the choice of $f = 0$, with the corresponding basis function $\phi$ in $W^{2.7816}$, and the other is the choice of $f = -\frac{10}{7^4}$, with the resulting $\phi \in W^{2.7865}$. In Table 1, we compile the $s_{\infty}(\phi)$ estimates of $\phi$ for $f = 0$ and $f = -\frac{10}{7^4}$. For the scheme with $f = 0$, we present the templates in Fig. 7. From Table 1, we can see that this is a $C^2$ subdivision scheme. With extensive experience by us and other researchers on computing Hölder exponents by joint spectral radius approximations, one might guess that the Hölder exponent should be 2.2971 for $f = 0$, and 2.3068 for $f = -\frac{10}{7^4}$. If
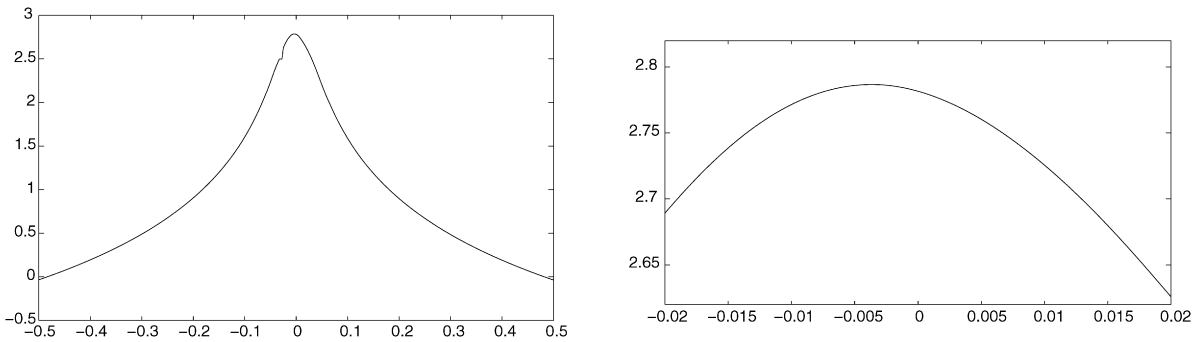
Fig. 6. Sobolev smoothness exponents of $\phi$ as a function of parameter $f$.
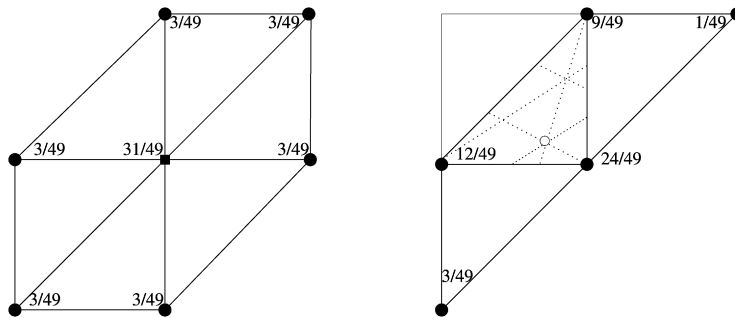


Fig. 7. $C^2$ approximation scalar $\sqrt{7}$-subdivision scheme.

Table 1
Hölder smoothness estimates for approximation scalar $\sqrt{7}$-subdivision schemes with $f = 0$ (with templates given in Fig. 7), $f = -\frac{10}{7^4}$, $g = h = j = k = m = n = 0$, and $x, y, a, b, c, d, e$ as given in (3.7)

| | $\ell$ | 1 | 2 | 3 | 4 | 5 | 6 | 7 | 8 | 9 |
|---|---|---|---|---|---|---|---|---|---|---|
| $f = 0$ | $\bar{s}^{\ell}_{\infty}(\phi)$ | 2.4171 | 2.2971 | 2.3833 | 2.2971 | 2.3779 | 2.2971 | 2.3755 | 2.2971 | 2.3728 |
| | $\underline{s}^{\ell}_{\infty}(\phi)$ | 0.3551 | 1.3051 | 1.7056 | 1.8172 | 1.9447 | 1.9786 | 2.0456 | 2.0583 | 2.1015 |
| $f = -\frac{10}{7^4}$ | $\bar{s}^{\ell}_{\infty}(\phi)$ | 2.4748 | 2.3086 | 2.4373 | 2.3086 | 2.4327 | 2.3086 | 2.4307 | 2.3086 | 2.4082 |
| | $\underline{s}^{\ell}_{\infty}(\phi)$ | −0.6076 | 0.8548 | 1.4062 | 1.6099 | 1.7732 | 1.8446 | 1.9268 | 1.9607 | 2.0117 |

we pay close attention to $\underline{s}^{\ell}_{\infty}(\phi)$, we find that $\underline{s}^{\ell}_{\infty}(\phi)$ is larger for $f = 0$ than for $f = -\frac{10}{7^4}$. This is perhaps due to the fact that since the subdivision mask of for $f = -\frac{10}{7^4}$ is larger, the estimate of $\underline{s}^{\ell}_{\infty}(\phi)$ for the corresponding basis function $\phi$ is less effective.

Next we would like to mention the scheme given by

$$x = 25/49, \quad y = 4/49, \quad a = 136/343, \quad b = 12/49, \quad c = 64/343, \quad d = 4/49,$$

$$e = 16/343, \quad f = 4/343, \quad g = 6/343, \quad h = 4/343, \quad k = 1/343.$$

This scheme has sum rule order 4 and its corresponding $\phi$ in $W^{3.8688}$, and this scheme is the composite subdivision scheme $S^2_{\text{lin}}$ introduced in [22]. Since the symbol is positive, we have $s_{\infty}(\phi) = \bar{s}^1_{\infty}(\phi)$. Therefore, $\phi$ is in $C^{3.2928}$.

### 3.1.2. Interpolatory $\sqrt{7}$-subdivision scalar templates

For a scalar subdivision scheme to be interpolatory, we need $x = 1$, $y = 0$. First we consider the schemes with reasonably small template sizes, by setting $g = h = j = k = m = n = 0$.

Again, with $x = 1$, $y = 0$, the solution of the linear system governed the sum rules yields a family of interpolatory masks that assures sum rule order 2, with parameters given by

$$a = 1 - c - b - e - d - f, \quad b = 2/7 - f + d - e, \quad c = 1/7 - d + e - f.$$

If we choose

$$d = -\frac{16}{343}, \quad e = -\frac{6}{343}, \quad f = -\frac{17}{343}$$

(and hence, $a = \frac{201}{343}$, $b = \frac{15}{49}$, $c = \frac{76}{343}$), then the corresponding $\phi$ is in $W^{1.7405}$ with Hölder smoothness estimates shown in Table 2. Although the Hölder smoothness order of this scheme seems to be too small from the lower-bound values $\underline{s}^{\ell}_{\infty}(\phi)$, we believe that the Hölder exponent of $\phi$ should be 1.0028 as given by the upper-bounds $\bar{s}^{\ell}_{\infty}(\phi)$. This is indeed justified by plots of the first divided differences from numerical discrete values of $\phi$, which suggest that $\phi$ is in $C^1$.

Next, we consider interpolatory schemes with a larger template size. With $x = 1$ and $y = 0$, the solution of the linear system governed by the sum rules yields a family of interpolatory masks of sum rule order 3 with parameters given by

$$a = 30/49 + 2(k + m - h - g) + n + j, \quad b = 18/49 + 2(g + n - j - k) + m + h,$$
$$c = 15/49 + 2(h + j - n - m) + g + k, \quad d = -3/49 - m - k - n - g,$$
$$e = -5/49 - j - m - k - h, \quad f = -6/49 - n - j - h - g. \tag{3.8}$$

When $m = k = j = n = 0$, if we choose $g = -8/343$, $h = -11/343$ (hence, $a = 248/343$, $b = 99/343$, $c = 75/343$, $d = -24/343$, $e = -13/343$, $f = -23/343$), then the resulting $\phi$ is in $W^{1.9734}$ with Hölder smoothness estimates shown in Table 3. We see that this is a $C^1$ scheme, and the template of this $C^1$ interpolatory subdivision scheme is displayed in Fig. 8.

Table 2
Hölder smoothness estimates for scalar interpolatory $\sqrt{7}$-subdivision scheme with $a = \frac{201}{343}$, $b = \frac{15}{49}$, $c = \frac{76}{343}$, $d = -\frac{16}{343}$, $e = -\frac{6}{343}$, $f = -\frac{17}{343}$, $g = h = j = k = m = n = 0$

| $\ell$ | 1 | 2 | 3 | 4 | 5 | 6 | 7 | 8 | 9 |
|---|---|---|---|---|---|---|---|---|---|
| $\bar{s}^{\ell}_{\infty}(\phi)$ | 1.0028 | 1.0028 | 1.0028 | 1.0028 | 1.0028 | 1.0028 | 1.0028 | 1.0028 | 1.0028 |
| $\underline{s}^{\ell}_{\infty}(\phi)$ | −1.1274 | 0.0734 | 0.3628 | 0.5297 | 0.6213 | 0.6859 | 0.7303 | 0.7646 | 0.7908 |

Table 3
Hölder smoothness estimates for interpolatory $\sqrt{7}$-subdivision scheme with templates in Fig. 8

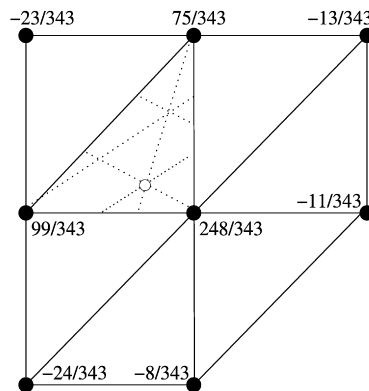| $\ell$ | 1 | 2 | 3 | 4 | 5 | 6 | 7 | 8 | 9 |
|---|---|---|---|---|---|---|---|---|---|
| $\bar{s}^{\ell}_{\infty}(\phi)$ | 1.7329 | 1.4623 | 1.6537 | 1.4623 | 1.6124 | 1.4623 | 1.5777 | 1.4623 | 1.5538 |
| $\underline{s}^{\ell}_{\infty}(\phi)$ | −1.3166 | 0.1698 | 0.6468 | 0.8153 | 0.9719 | 1.0293 | 1.1116 | 1.1373 | 1.1895 |



Fig. 8. $C^1$ interpolatory $\sqrt{7}$-subdivision scheme.

Finally, we present an interpolatory scheme with larger template size to achieve a higher order of smoothness. For the choice of

$$[n, j, m, h, k, g] = \frac{1}{7^4}[-26, -33, -26, -72, -62, -90], \tag{3.9}$$

the resulting $\phi \in W^{2.57786}$. From the Hölder smoothness estimates (not provided here), we see that this scheme is still not $C^2$ yet.

To construct $C^2$ interpolatory schemes, we need to consider templates, with size so large that no longer have any practical value. In the next subsection we will construct $C^2$ vector interpolatory schemes with significantly smaller template sizes.

## 3.2. Vector $\sqrt{7}$-subdivision schemes

The general templates for the (approximation and interpolatory) vector $\sqrt{7}$-subdivision schemes are shown in Fig. 9, where $X, Y, L, B, C, D, E, F$ are $2 \times 2$ matrices. The corresponding subdivision mask $\{P_{\mathbf{k}}\}$ is given by the following block-matrix in (3.10), whose $(k_1, k_2)$-block is $P_{k_2-5, -(k_1-5)}$, to match the notation in (1.2), where the dilation matrix $A$ is given by the matrix $M$ in (3.3).

$$\begin{bmatrix} \mathbf{0} & \mathbf{0} & \mathbf{0} & \mathbf{0} & \mathbf{0} & \mathbf{0} & \mathbf{0} & F & \mathbf{0} \\ \mathbf{0} & \mathbf{0} & \mathbf{0} & F & E & Y & D & E & \mathbf{0} \\ \mathbf{0} & \mathbf{0} & \mathbf{0} & D & C & B & C & Y & \mathbf{0} \\ \mathbf{0} & \mathbf{0} & Y & B & L & L & B & D & F \\ \mathbf{0} & E & C & L & \mathbf{X} & L & C & E & \mathbf{0} \\ F & D & B & L & L & B & Y & \mathbf{0} & \mathbf{0} \\ \mathbf{0} & Y & C & B & C & D & \mathbf{0} & \mathbf{0} & \mathbf{0} \\ \mathbf{0} & E & D & Y & E & F & \mathbf{0} & \mathbf{0} & \mathbf{0} \\ \mathbf{0} & F & \mathbf{0} & \mathbf{0} & \mathbf{0} & \mathbf{0} & \mathbf{0} & \mathbf{0} & \mathbf{0} \end{bmatrix}. \tag{3.10}$$

### 3.2.1. Approximation $\sqrt{7}$-subdivision matrix templates

First let us study approximation schemes. By solving the linear system (2.4) for the matrix-valued mask with $\eta_j$ as in (3.4) and $\mathbf{y}_\alpha$ in (2.5) given by

$$\mathbf{y}_{0,0} = [1, 0], \quad \mathbf{y}_{1,0} = \mathbf{y}_{0,1} = [0, 0], \quad \mathbf{y}_{2,0} = \mathbf{y}_{0,2} = [0, 1], \quad \mathbf{y}_{1,1} = \left[0, \frac{1}{2}\right], \tag{3.11}$$

we have a family of matrix-valued masks for sum rule order 3, given by

$$X = \begin{bmatrix} 1 - 6y_{11} & -6y_{12} \\ -4y_{11} - 6y_{21} & \frac{1}{7} - 4y_{12} - 6y_{22} \end{bmatrix}, \quad Y = \begin{bmatrix} y_{11} & y_{12} \\ y_{21} & y_{22} \end{bmatrix},$$

$$L = \begin{bmatrix} \frac{24}{49} - f_{11} & -f_{12} \\ -\frac{12}{49} - 2f_{11} - b_{21} - c_{21} - d_{21} - e_{21} - f_{21} & \frac{1}{7} - 2f_{12} - b_{22} - c_{22} - d_{22} - e_{22} - f_{22} \end{bmatrix},$$
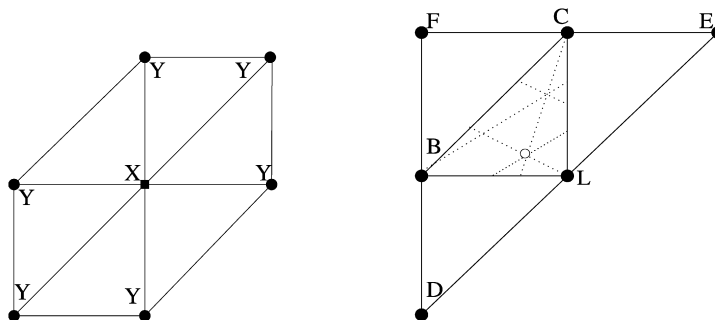


Fig. 9. Templates for (approximation and interpolatory) vector $\sqrt{7}$-subdivision schemes.

Table 4
Hölder smoothness estimates for approximation vector $\sqrt{7}$-subdivision scheme with parameters given by (3.14)

| $\ell$ | 1 | 2 | 3 | 4 | 5 | 6 | 7 | 8 | 9 |
|---|---|---|---|---|---|---|---|---|---|
| $\bar{s}^\ell_\infty(\Phi)$ | 2.6496 | 2.6496 | 2.6496 | 2.6496 | 2.6496 | 2.6496 | 2.6496 | 2.6496 | 2.6496 |
| $\underline{s}^\ell_\infty(\Phi)$ | $-2.1813$ | 0.4407 | 1.0731 | 1.51755 | 1.7297 | 1.9085 | 2.0107 | 2.0936 | 2.2332 |

$$B = \begin{bmatrix} \frac{12}{49} - f_{11} & -f_{12} \\ b_{21} & b_{22} \end{bmatrix}, \quad C = \begin{bmatrix} \frac{9}{49} - f_{11} & -f_{12} \\ c_{21} & c_{22} \end{bmatrix},$$

$$D = \begin{bmatrix} \frac{3}{49} + f_{11} & f_{12} \\ d_{21} & d_{22} \end{bmatrix}, \quad E = \begin{bmatrix} \frac{1}{49} + f_{11} & f_{12} \\ e_{21} & e_{22} \end{bmatrix}, \quad F = \begin{bmatrix} f_{11} & f_{12} \\ f_{21} & f_{22} \end{bmatrix}. \tag{3.12}$$

When $F = \mathbf{0}$, we may choose the parameters (which are not provided here to save space) such that the corresponding $\Phi$ is in $W^{2.8441}$. For the purpose of integer implementations, we choose

$$[y_{11}, y_{12}, y_{21}, y_{22}, b_{21}, b_{22}, c_{21}, c_{22}, d_{21}, d_{22}, e_{21}, e_{22}]$$
$$= \frac{1}{7^4}[171, 423, -66, -202, -159, 86, -127, 77, -21, 25, -53, 39]. \tag{3.13}$$

Then the corresponding $\Phi$ is in $W^{2.8434}$.

More generally, when $F = \mathbf{0}$ in not imposed, there exist parameters (not provided here to save space), such that the corresponding $\Phi$ is in $W^{2.9952}$. For the purpose of integer (or fixed point) implementations, we choose

$$[y_{11}, y_{12}, y_{21}, y_{22}, b_{21}, b_{22}, c_{21}, c_{22}, d_{21}, d_{22}, e_{21}, e_{22}, f_{11}, f_{12}, f_{21}, f_{22}]$$
$$= \frac{1}{7^4}[192, 418, -79, -224, -159, 72, -125, 77, -27, 32, -59, 59, 22, 14, -19, -11]. \tag{3.14}$$

Then the corresponding $\Phi$ is in $W^{2.9942}$, with Hölder smoothness estimates shown in Table 4. From Table 4, we see that this is a $C^2$ scheme.

The matrix-valued subdivision masks constructed above satisfy the sum rule of order 3. If we want a matrix-valued mask to satisfy sum rule of order 4, then we need to use templates of larger sizes. Fortunately, as shown above, masks that satisfy the sum rule of order 3 are good enough for the purpose of constructing $C^2$ subdivision schemes. Therefore, we will not consider matrix-valued $\sqrt{7}$-subdivision masks with sum rule of order 4 or higher.

### 3.2.2. Interpolatory $\sqrt{7}$-subdivision matrix templates

Let $X, Y, L, B, C, D, E, F$ be the matrices as given in (3.12). Then by choosing

$$y_{11} = 0, \quad y_{21} = 0,$$

$X, Y$ become

$$X = \begin{bmatrix} 1 & -6y_{12} \\ 0 & \frac{1}{7} - 4y_{12} - 6y_{22} \end{bmatrix}, \quad Y = \begin{bmatrix} 0 & y_{12} \\ 0 & y_{22} \end{bmatrix},$$

so that the corresponding mask $\{P_\mathbf{k}\}$ satisfies the interpolatory condition (1.5). It is clear from the previous subsection that the interpolatory mask also satisfies the sum rule of order 3 with the vectors $\mathbf{y}_\alpha$ given in (3.11).

In particular, for $F = \mathbf{0}$, there exist parameters (not provided here to save space), such that the corresponding refinable function vector $\Phi$ is in $W^{2.6256}$. For integer implementations, we choose

$$[y_{21}, y_{22}, b_{21}, b_{22}, c_{21}, c_{22}, d_{21}, d_{22}, e_{21}, e_{22}]$$
$$= \frac{1}{7^4}[2059/4, -150, -167, 94, -118, 38, -14, -15, -36, -27]. \tag{3.15}$$

Then $\Phi$ is in $W^{2.6253}$.

Without assuming $F = \mathbf{0}$, there exist parameters (not provided here to save space) to yield an even smoother refinable function vector $\Phi$ in $W^{2.9037}$. For integer implementations, we choose

Table 5
Hölder smoothness estimates for interpolatory vector $\sqrt{7}$-subdivision scheme with parameters given by (3.16)

| $\ell$ | 1 | 2 | 3 | 4 | 5 | 6 | 7 | 8 | 9 |
|---|---|---|---|---|---|---|---|---|---|
| $\bar{s}_\infty^\ell(\Phi)$ | 2.5371 | 2.5371 | 2.5371 | 2.5371 | 2.5371 | 2.5371 | 2.5371 | 2.5371 | 2.5371 |
| $\underline{s}_\infty^\ell(\Phi)$ | −1.7109 | 0.2956 | 1.0054 | 1.3467 | 1.5600 | 1.6948 | 1.8546 | 1.9535 | 2.0248 |

$$[y_{21}, y_{22}, b_{21}, b_{22}, c_{21}, c_{22}, d_{21}, d_{22}, e_{21}, e_{22}, f_{11}, f_{12}, f_{21}, f_{22}]$$
$$= \frac{1}{7^4}[1101/2, -171, -174, 90, -128, 34, -18, -13, -43, -19, 16, 22, -5, -7]. \tag{3.16}$$

Then $\Phi$ is in $W^{2.8945}$, with Hölder smoothness estimates shown in Table 5. From Table 5, we see that this is a $C^2$ scheme.

## 4. $\sqrt{5}$-Subdivision schemes

First we need to find an appropriate dilation matrix $A$ for the $\sqrt{5}$-subdivision. Again, such dilation matrices should have integer entries and that their inverses should map the coarse mesh onto one of the finer meshes, shown in Fig. 4. There are many such matrices, such as

$$\pm \begin{bmatrix} 1 & -2 \\ 2 & 1 \end{bmatrix}, \quad \pm \begin{bmatrix} 1 & 2 \\ -2 & 1 \end{bmatrix}, \quad \pm \begin{bmatrix} 2 & -1 \\ 1 & 2 \end{bmatrix}, \quad \pm \begin{bmatrix} 2 & 1 \\ -1 & 2 \end{bmatrix}, \tag{4.1}$$

and

$$\pm \begin{bmatrix} 2 & 1 \\ 1 & -2 \end{bmatrix}, \quad \pm \begin{bmatrix} -2 & 1 \\ 1 & 2 \end{bmatrix}, \quad \pm \begin{bmatrix} 1 & 2 \\ 2 & -1 \end{bmatrix}, \quad \pm \begin{bmatrix} -1 & 2 \\ 2 & 1 \end{bmatrix}. \tag{4.2}$$

Observe that the dilation matrices in the second list (4.2) satisfy $A^2 = 5I_2$. In the following, we will choose the matrix

$$N := \begin{bmatrix} 2 & 1 \\ 1 & -2 \end{bmatrix} \tag{4.3}$$

from the second list as the dilation matrix for our study of $\sqrt{5}$-subdivisions and consider the finer mesh on the left of Fig. 4. For this dilation matrix $N$, the choice of

$$\eta_0 = (0, 0), \quad \eta_1 = (1, 0), \quad \eta_2 = (0, 1), \quad \eta_3 = (-1, 0), \quad \eta_4 = (0, -1), \tag{4.4}$$

yields 5 distinct elements $\eta_j + N^T \mathbb{Z}^2$, $j = 0, \ldots, 4$, of $\mathbb{Z}^2/(N^T \mathbb{Z}^2)$. Both scalar and vector $\sqrt{5}$-subdivision schemes will be constructed in the next subsections.

### 4.1. Scalar $\sqrt{5}$-subdivision schemes

The general templates for the local averaging rules are shown in Fig. 10. In particular, interpolating schemes are achieved by setting $x = 1$, $y = 0$ and $z = 0$. Observe that the corresponding subdivision mask $\{p_{\mathbf{k}}\}$ is given by the following matrix in (4.5), whose $(k_1, k_2)$-entry matches with $p_{k_2-5, -(k_1-5)}$.

$$\begin{bmatrix} 0 & 0 & 0 & k & m & 0 & 0 & 0 & 0 \\ 0 & n & j & f & g & z & h & n & 0 \\ 0 & h & e & y & d & c & e & j & 0 \\ 0 & z & c & b & a & b & y & f & k \\ m & g & d & a & \mathbf{x} & a & d & g & m \\ k & f & y & b & a & b & c & z & 0 \\ 0 & j & e & c & d & y & e & h & 0 \\ 0 & n & h & z & g & f & j & n & 0 \\ 0 & 0 & 0 & 0 & m & k & 0 & 0 & 0 \end{bmatrix}. \tag{4.5}$$
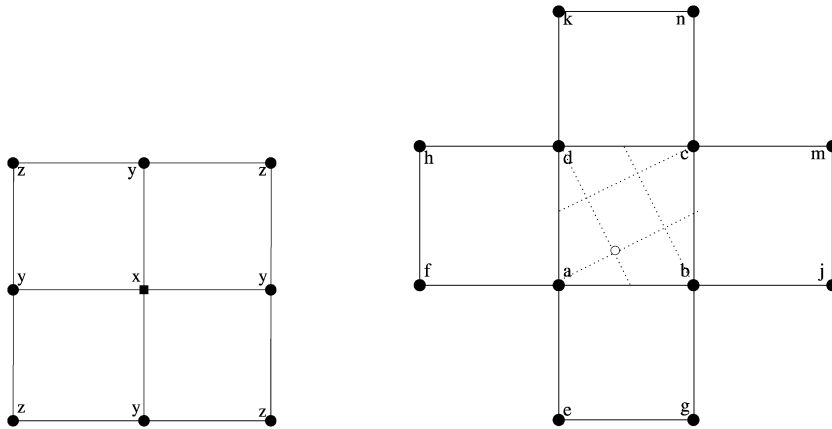
Fig. 10. Templates for scalar $\sqrt{5}$-subdivision schemes.

Table 6
Hölder smoothness estimates for the scalar approximation $\sqrt{5}$-subdivision scheme in [11]

| $\ell$ | 1 | 2 | 3 | 4 | 5 | 6 | 7 | 8 | 9 |
|---|---|---|---|---|---|---|---|---|---|
| $\bar{s}^\ell_\infty(\phi)$ | 1.2829 | 1.2829 | 1.2829 | 1.2829 | 1.2829 | 1.2829 | 1.2829 | 1.2829 | 1.2829 |
| $\underline{s}^\ell_\infty(\phi)$ | $-3.4428$ | $-1.1394$ | $-0.3565$ | 0.0547 | 0.3091 | 0.4787 | 0.6018 | 0.6941 | 0.7667 |

Table 7
Hölder smoothness estimates for approximation $\sqrt{5}$-subdivision scheme with templates in Fig. 11

| $\ell$ | 1 | 2 | 3 | 4 | 5 | 6 | 7 | 8 | 9 |
|---|---|---|---|---|---|---|---|---|---|
| $\bar{s}^\ell_\infty(\phi)$ | 1.6425 | 1.6425 | 1.6425 | 1.6425 | 1.6425 | 1.6425 | 1.6425 | 1.6425 | 1.6425 |
| $\underline{s}^\ell_\infty(\phi)$ | $-3.0579$ | $-0.9530$ | $-0.1279$ | 0.3638 | 0.6350 | 0.8201 | 0.9537 | 1.0530 | 1.1331 |

### 4.1.1. Approximation $\sqrt{5}$-subdivision scalar templates

First we consider subdivision schemes with small template sizes, by setting $z = 0$, $e = f = g = h = j = k = m = n = 0$. Let $\{p_{\mathbf{k}}\}$ be the corresponding mask and $p(\omega) = \frac{1}{5}\sum_{\mathbf{k}} p_{\mathbf{k}} e^{-i\mathbf{k}\omega}$. We may eliminate some of the parameters $a, b, c, d, x, y$ by considering masks $\{p_{\mathbf{k}}\}$ with sum rule of order 2 only, namely: the solution of the linear system governed by

$$p(0) = 1, \qquad D^\mu p\big(2\pi N^{-T}\eta_j\big) = 0, \quad j = 1, \ldots, 4, \ |\mu| < 2, \tag{4.6}$$

with $\eta_j$ given by (4.4), yields a family of masks of sum rule order 2, satisfying:

$$a = 3/5 - d, \quad c = 1/5 - d, \quad b = 1/5 + d, \quad x = 1 - 4y.$$

In [11], the authors chose $y = 1/5$, $d = 1/10$ (and hence, $x = 1/5$, $a = 1/2$, $b = 3/10$, $c = 1/10$). The reason for such choices is that the authors of [11] tried to force the fourth leading eigenvalue of the corresponding subdivision matrix $S$ to be $\frac{1}{5}$, which happens to be the product of the second and third leading eigenvalues $\frac{1}{\sqrt{5}}i$, $-\frac{1}{\sqrt{5}}i$. (Observe that the $C^1$ condition implies that $1$, $\frac{1}{\sqrt{5}}i$, $-\frac{1}{\sqrt{5}}i$ are the leading eigenvalues of $S$.) For this scheme, we see that the corresponding basis function $\phi$ is in $W^{1.5539}$, with $s_\infty(\phi)$ estimates shown in Table 6. On the other hand, by choosing

$$y = 1/10, \quad d = 2/15$$

(and hence, $x = 3/5$, $a = 7/15$, $b = 1/3$, $c = 1/15$), we have a smoother refinable function $\phi \in W^{1.9713}$, with $s_\infty(\phi)$ estimates $\phi$ shown in Table 7. Therefore, the choice of $y = 1/10$ and $d = 2/15$ provides a smoother $C^1$ $\sqrt{5}$-subdivision scheme with templates of the same size as those in [11]. The subdivision templates of our $C^1$ scheme are displayed in Fig. 11.
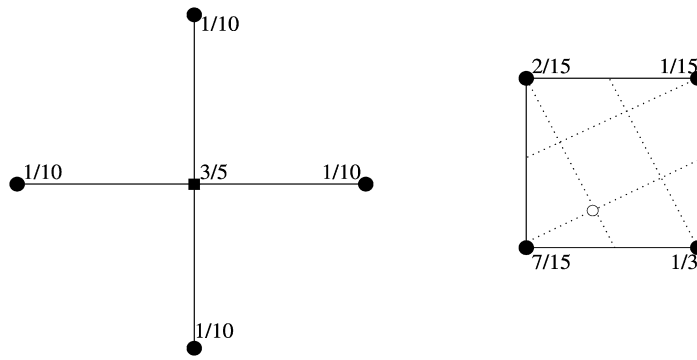
Fig. 11. $C^1$ approximation $\sqrt{5}$-subdivision scheme.

Table 8
Hölder smoothness estimates for approximation $\sqrt{5}$-subdivision scheme with templates in Fig. 12

| $\ell$ | 1 | 2 | 3 | 4 | 5 | 6 | 7 | 8 | 9 |
|---|---|---|---|---|---|---|---|---|---|
| $\bar{s}_\infty^\ell(\phi)$ | 2.7080 | 2.4063 | 2.5171 | 2.4063 | 2.4728 | 2.4063 | 2.4538 | 2.4063 | 2.4432 |
| $\underline{s}_\infty^\ell(\phi)$ | $-1.8490$ | $-0.2444$ | 0.5605 | 1.0489 | 1.3413 | 1.5068 | 1.6466 | 1.7297 | 1.8134 |

Table 9
Hölder smoothness estimates for scalar approximation $\sqrt{5}$-subdivision scheme with $x = 61/125$, $y = 16/125$, $a = 46/125$, $b = 41/125$, $c = 2/25$, $d = 21/125$, $e = 6/125$, $f = 1/125$, and $z = g = h = j = k = m = n = 0$

| $\ell$ | 1 | 2 | 3 | 4 | 5 | 6 | 7 | 8 | 9 |
|---|---|---|---|---|---|---|---|---|---|
| $\bar{s}_\infty^\ell(\phi)$ | 2.6442 | 2.4966 | 2.6308 | 2.4966 | 2.5779 | 2.4966 | 2.5551 | 2.4966 | 2.5423 |
| $\underline{s}_\infty^\ell(\phi)$ | $-1.7882$ | $-0.1995$ | 0.6048 | 1.1195 | 1.4343 | 1.6003 | 1.7400 | 1.8239 | 1.9057 |

Next let us construct subdivision schemes with slightly larger templates to gain higher order of smoothness, by allowing $e$, $f$ to be non-zero (though $z = 0$ and $g = h = j = k = m = n = 0$). Then by solving the linear system governed by the sum rules, we obtain a family of masks of sum rule order 3, with parameters given by

$$x = 13/25 - 4f, \quad y = 3/25 + f, \quad a = 2/5 - 4f, \quad b = 8/25 + f,$$
$$c = 2/25, \quad d = 4/25 + f, \quad e = 1/25 + f. \tag{4.7}$$

For $f = 0$, the corresponding refinable $\phi$ is in $W^{2.8637}$ with $s_\infty(\phi)$ estimates shown in Table 8. For $f = 1/125$, we have $\phi \in W^{2.9015}$ with $s_\infty(\phi)$ estimates shown in Table 9. Though the estimates of $\underline{s}_\infty^\ell(\phi)$ in Tables 8 and 9 cannot be used to justify that these two subdivision schemes are $C^2$ schemes, we believe that they are actually $C^2$, judging from the pictures of the second order partial derivatives of the basis functions. The templates for the scheme with $f = 0$ are displayed in Fig. 12.

Finally, let us consider the following particular choices of parameters:

$$[x, y, z, a, b, c, d, e, f, g, m, j, h, k, n]$$
$$= \frac{1}{125}[61, 12, 4, 40, 36, 12, 22, 6, 4, 4, 1, 0, 0, 0, 0], \tag{4.8}$$

with corresponding symbol

$$p_{\text{comp}}(\omega) = \frac{1}{25}\left(1 + \frac{2}{5}\left(z_1 + z_2 + \frac{1}{z_1} + \frac{1}{z_2}\right) + \frac{2}{5}\left(z_1 z_2 + \frac{1}{z_1 z_2} + \frac{z_1}{z_2} + \frac{z_2}{z_1}\right) + \frac{1}{5}\left(z_1^2 + z_2^2 + \frac{1}{z_1^2} + \frac{1}{z_2^2}\right)\right)^2,$$

where $z_1 = e^{-i\omega_1}$, $z_2 = e^{-i\omega_2}$. This symbol satisfies the sum rule of order 4. Analogous to the study of $\sqrt{7}$-subdivision schemes in [22], the subdivision scheme corresponding to the symbol $p_{\text{comp}}(\omega)$ can be described as a composite
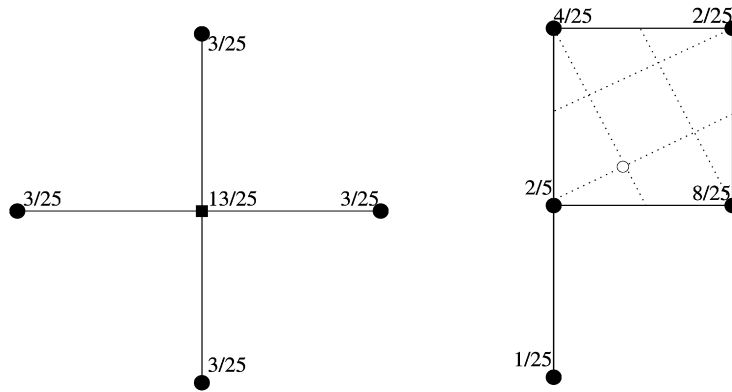
Fig. 12. "$C^2$" approximation $\sqrt{5}$-subdivision scheme.

$\sqrt{5}$-subdivision scheme, with basis function $\phi \in W^{2.5389}$. Since $p_{\text{comp}}(\omega) \geqslant 0$, we have $s_\infty(\phi) = \bar{s}_\infty^1(\phi) = 2.4634$. Thus, $\phi$ is in $C^{2.4634}$.

We remark that the non-zero coefficients $p_{\mathbf{k}}$ in all of the above subdivision schemes are positive.

### 4.1.2. Interpolatory $\sqrt{5}$-subdivision scalar templates

For the subdivision schemes to be interpolatory, we must set $x = 1$, $y = z = 0$. Consider

$$a = 61/125, \quad b = 39/125, \quad c = 11/125, \quad d = 14/125,$$
$$e = f = g = h = j = k = m = n = 0. \tag{4.9}$$

Then the corresponding mask satisfies the sum rule of order 2, with $\phi \in W^{1.6496}$. From the Hölder smoothness estimates of this subdivision scheme (not provided here), we see that this scheme is probably not $C^1$. For this reason, we consider slightly larger templates.

By solving the linear system governed by the sum rules, we obtain a family of masks of sum rule order 3, with parameters given by

$$a = 22/25 + 2g + 2h + 3j + 3k + 2m + 2n, \quad b = 1/5 - h - 2g - 3j - m + n,$$
$$c = 2/25 + g + h - 2m - 2n, \quad d = 1/25 - g - 2h - n - 3k + m,$$
$$e = -2/25 - g - n - k, \quad f = -3/25 - h - j - m. \tag{4.10}$$

For the case $j = k = m = n = 0$, by choosing

$$g = -10/125, \quad h = -3/125, \tag{4.11}$$

we have $\phi \in W^{1.7337}$. from the Hölder smoothness estimates, we see the order of smoothness of this scheme is still too small.

Next, we choose

$$[g, h, j, k, m, n] = \frac{1}{5^4}[7, 11, 31, 6, 2, 13], \tag{4.12}$$

so that

$$[a, b, c, d, e, f] = \frac{1}{5^4}[373, 232, 62, 83, -24, -31]. \tag{4.13}$$

Then we have $\phi \in W^{2.6030}$, which assures that this subdivision scheme is a $C^1$ interpolatory scheme. From the Hölder smoothness estimates of $\phi$, we know that this is not a $C^2$ scheme.
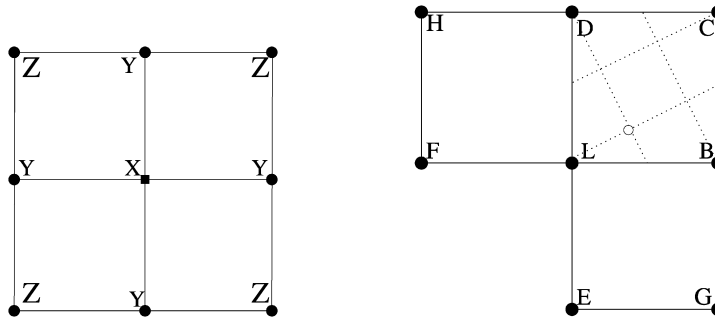
Fig. 13. Templates for (approximation and interpolatory) vector $\sqrt{5}$-subdivision schemes.

## 4.2. Vector $\sqrt{5}$-subdivision schemes

The general subdivision templates for both approximation and interpolatory vector $\sqrt{5}$-subdivision schemes are shown in Fig. 13, where $X, Y, Z, L, B, C, D, E, F, G, H$ are $2 \times 2$ matrices. The corresponding subdivision mask $\{P_{\mathbf{k}}\}$ is given by the following block-matrix in (4.14), whose $(k_1, k_2)$-block entry is $P_{k_2-4, -(k_1-4)}$.

$$\begin{bmatrix} \mathbf{0} & \mathbf{0} & F & G & Z & H & \mathbf{0} \\ H & E & Y & D & C & E & \mathbf{0} \\ Z & C & B & L & B & Y & F \\ G & D & L & \mathbf{X} & L & D & G \\ F & Y & B & L & B & C & Z \\ \mathbf{0} & E & C & D & Y & E & H \\ \mathbf{0} & H & Z & G & F & \mathbf{0} & \mathbf{0} \end{bmatrix}. \tag{4.14}$$

### 4.2.1. Approximation $\sqrt{5}$-subdivision matrix templates

We first consider small templates by setting $Z = G = H = \mathbf{0}$. Then solving the linear system (2.4) for the matrix-valued mask with $\eta_j$ as in (4.4) and $\mathbf{y}_\alpha$ in (2.5) given by

$$\mathbf{y}_{0,0} = [1, 0], \quad \mathbf{y}_{1,0} = \mathbf{y}_{0,1} = [0, 0], \quad \mathbf{y}_{2,0} = \mathbf{y}_{0,2} = [0, 1], \quad \mathbf{y}_{1,1} = [0, 0], \tag{4.15}$$

we obtain a family of matrix-valued masks of sum rule order 3, given by

$$X = \begin{bmatrix} 1 - 4y_{11} & -4y_{12} \\ -2y_{11} - 4y_{21} & \frac{1}{5} - 2y_{12} - 4y_{22} \end{bmatrix}, \quad Y = \begin{bmatrix} y_{11} & y_{12} \\ y_{21} & y_{22} \end{bmatrix},$$

$$L = \begin{bmatrix} \frac{2}{5} - 4f_{11} + 2g_{11} - 2h_{11} & -4f_{12} \\ -\frac{6}{25} - 2f_{11} - b_{21} - c_{21} - d_{21} - e_{21} - f_{21} & \frac{1}{5} - 2f_{12} - b_{22} - c_{22} - d_{22} - e_{22} - f_{22} \end{bmatrix},$$

$$B = \begin{bmatrix} \frac{8}{25} + f_{11} & f_{12} \\ b_{21} & b_{22} \end{bmatrix}, \quad C = \begin{bmatrix} \frac{2}{25} & 0 \\ c_{21} & c_{22} \end{bmatrix},$$

$$D = \begin{bmatrix} \frac{4}{25} + f_{11} & f_{12} \\ d_{21} & d_{22} \end{bmatrix}, \quad E = \begin{bmatrix} \frac{1}{25} + f_{11} - g_{11} + h_{11} & f_{12} \\ e_{21} & e_{22} \end{bmatrix}, \quad F = \begin{bmatrix} f_{11} & f_{12} \\ f_{21} & f_{22} \end{bmatrix}. \tag{4.16}$$

For a smaller template with $F = \mathbf{0}$, there exist parameters (not provided here to save space) such that the resulting $\Phi$ is in $W^{2.9084}$. Even for integer implementations with

$$[y_{11}, y_{12}, y_{21}, y_{22}, b_{21}, b_{22}, c_{21}, c_{22}, d_{21}, d_{22}, e_{21}, e_{22}]$$
$$= \frac{1}{5^4}[126, 181, -49, -93, -54, 19, -13, 14, -23, 31, 3, 27], \tag{4.17}$$

we already have $\Phi \in W^{2.9045}$. From the Hölder smoothness estimates, we know it is a $C^2$ scheme.

Next, we consider the subdivision masks that satisfy the sum rule of the higher order 4, with $Z = \mathbf{0}$ but no restriction on $F, G, H$. For the choices of

$$X = \begin{bmatrix} 1 - 4y_{11} & -4y_{12} \\ -2y_{11} - 4y_{21} & \frac{1}{5} - 2y_{12} - 4y_{22} \end{bmatrix}, \quad Y = \begin{bmatrix} y_{11} & y_{12} \\ y_{21} & y_{22} \end{bmatrix},$$

$$L = \begin{bmatrix} \frac{54}{125} - 4f_{11} & -4f_{12} \\ -\frac{18}{125} - 2f_{11} - d_{21} - e_{21} - 2f_{21} - 2h_{21} & \frac{3}{25} - 2f_{12} - d_{22} - e_{22} - 2f_{22} - 2h_{22} \end{bmatrix},$$

$$B = \begin{bmatrix} \frac{34}{125} + f_{11} & f_{12} \\ -6/125 + d_{21} - e_{21} + f_{21} - 2g_{21} + 2h_{21} & 1/25 + d_{22} - e_{22} + f_{22} - 2g_{22} + 2h_{22} \end{bmatrix},$$

$$C = \begin{bmatrix} \frac{4}{125} & 0 \\ -8/125 - d_{21} + e_{21} + g_{21} - h_{21} & 1/25 - d_{22} + e_{22} + g_{22} - h_{22} \end{bmatrix},$$

$$D = \begin{bmatrix} \frac{16}{125} + f_{11} & f_{12} \\ d_{21} & d_{22} \end{bmatrix}, \quad E = \begin{bmatrix} \frac{3}{125} + f_{11} & f_{12} \\ e_{21} & e_{22} \end{bmatrix}, \quad F = \begin{bmatrix} f_{11} & f_{12} \\ f_{21} & f_{22} \end{bmatrix},$$

$$G = \begin{bmatrix} 3/125 & 0 \\ g_{21} & g_{22} \end{bmatrix}, \quad H = \begin{bmatrix} 1/125 & 0 \\ h_{21} & h_{22} \end{bmatrix}, \tag{4.18}$$

we have a family of subdivision masks which satisfy the sum rule of order 4 with the vectors $\mathbf{y}_\alpha$ in (2.4) or (2.6) given by (4.15) and

$$\mathbf{y}_{3,0} = \mathbf{y}_{2,1} = \mathbf{y}_{1,2} = \mathbf{y}_{0,3} = [0, 0]. \tag{4.19}$$

Although there exist parameters (not provided here to save space) such that the resulting $\Phi$ is in $W^{3.8063}$, we prefer integer implementations with

$$[y_{11}, y_{12}, y_{21}, y_{22}, d_{21}, d_{22}, e_{21}, e_{22}, f_{11}, f_{12}, f_{21}, f_{22}, g_{21}, g_{22}, h_{21}, h_{22}]$$
$$= \frac{1}{5^4}[90, 54, -26, -13, -35, -10, -16, -27, 24, 61, -10, -26, -6, 3, -4, -3],$$

with corresponding $\Phi \in W^{3.7489}$. Since $\Phi$ is already in $C^2$, there is no need to provide the Hölder smoothness estimates here.

### 4.2.2. Interpolatory $\sqrt{5}$-subdivision matrix templates

First we consider smaller templates by setting $G = H = \mathbf{0}$. Let $L, B, C, D, E, F$ be the matrices as given in (4.16), and $X, Y, Z$ chosen to be

$$X = \begin{bmatrix} 1 & -4y_{12} - 4y_{12} \\ 0 & \frac{1}{5} - 2y_{12} - 4y_{22} - 4z_{12} - 4z_{22} \end{bmatrix}, \quad Y = \begin{bmatrix} 0 & y_{12} \\ 0 & y_{22} \end{bmatrix}, \quad Z = \begin{bmatrix} 0 & z_{12} \\ 0 & z_{22} \end{bmatrix}. \tag{4.20}$$

Then the corresponding subdivision masks satisfy (1.5), and hence, the subdivision schemes are interpolatory. These interpolatory masks also satisfy the sum rule of order 3 with vectors $\mathbf{y}_\alpha$ given in (4.15). Although there exist parameters (not provided here to save space) such that the resulting $\Phi$ is in $W^{2.6230}$, we prefer integer implementations with

$$[y_{12}, y_{22}, b_{21}, b_{22}, c_{21}, c_{22}, d_{21}, d_{22}, e_{21}, e_{22}, z_{12}, z_{22}, f_{11}, f_{12}, f_{21}, f_{22}]$$
$$= \frac{1}{5^4}[169, -53, -36, 32, -21, 10, -16, -5, -1, -13, 65, -23, -26, 34, 5, -9], \tag{4.21}$$

for which the corresponding $\Phi$ is in $W^{2.6172}$.

Finally, we construct interpolatory subdivision masks with the higher sum rule order 4, by allowing $F, G, H$ to be non-zero. For $L, B, C, D, E, F, G, H$ as given in (4.18) and $X, Y, Z$ given in (4.20), we do have interpolatory subdivision masks that satisfy the sum rule of order 4, with vectors $\mathbf{y}_\alpha$ given in (4.15) and (4.19). Although there exist parameters (not provided here to save space) such that the resulting $\Phi$ is in $W^{3.4378}$, we prefer integer implementations with

$$[y_{12}, y_{22}, d_{21}, d_{22}, e_{21}, e_{22}, f_{11}, f_{12}, f_{21}, f_{22}, g_{21}, g_{22}, h_{21}, h_{22}, z_{12}, z_{22}]$$
$$= \frac{1}{5^4}[216, -73, -26, 10, -4, -5, -5, 8, 1, -3, -4, -3, -1, -2, 68, -21],$$

for which $\Phi \in W^{3.3787}$, so that $\Phi$ is already in $C^2$.

## References

[1] E. Catmull, J. Clark, Recursively generated B-splines surfaces on arbitrary topological meshes, Comput. Aided Geom. Design 10 (1978) 350–355.

[2] C.K. Chui, Q.T. Jiang, Surface subdivision schemes generated by refinable bivariate spline function vectors, Appl. Comput. Harmon. Anal. 15 (2003) 147–162.

[3] C.K. Chui, Q.T. Jiang, Refinable bivariate $C^2$-splines for multi-level data representation and surface display, Math. Comp. 74 (2005) 1369–1390.

[4] C.K. Chui, Q.T. Jiang, Matrix-valued symmetric templates for interpolatory surface subdivisions, I: Regular vertices, Appl. Comput. Harmon. Anal. 19 (2005) 303–339.

[5] C.K. Chui, Q.T. Jiang, Matrix-valued subdivision schemes for generating surfaces with extraordinary vertices, Comput. Aided Geom. Design 23 (2006) 419–438.

[6] C.K. Chui, Q.T. Jiang, Refinable bivariate quartic and quintic $C^2$-splines for quadrilateral subdivisions, J. Comput. Appl. Math. 196 (2006) 402–424.

[7] N. Dyn, D. Levin, J.A. Gregory, A butterfly subdivision scheme for surface interpolation with tension control, ACM Trans. Graphics 2 (1990) 160–169.

[8] B. Han, R.Q. Jia, Multivariate refinement equations and convergence of subdivision schemes, SIAM J. Math. Anal. 29 (1998) 1177–1999.

[9] B. Han, R.Q. Jia, Quincunx fundamental refinable functions and quincunx biorthogonal wavelets, Math. Comp. 71 (2002) 165–196.

[10] I.P. Ivrissimtzis, N.A. Dodgson, M.F. Hassan, M.A. Sabin, On the geometry of recursive subdivision, Internat. J. Shape Modeling 8 (2002) 23–42.

[11] I.P. Ivrissimtzis, M.A. Sabin, N.A. Dodgson, $\sqrt{5}$-subdivision, in: Advances in Multiresolution for Geometric Modelling, Springer, 2005, pp. 285–299.

[12] H. Ji, S.D. Riemenschneider, Z.W. Shen, Multivariate compactly supported fundamental refinable functions, duals, and biorthogonal wavelets, Stud. Appl. Math. 102 (1999) 173–204.

[13] R.Q. Jia, Q.T. Jiang, Approximation power of refinable vectors of functions, in: Wavelet Analysis and Applications, in: AMS/IP Stud. Adv. Math., vol. 25, Amer. Math. Soc., Providence, RI, 2002, pp. 155–178.

[14] R.Q. Jia, Q.T. Jiang, Spectral analysis of transition operators and its applications to smoothness analysis of wavelets, SIAM J. Matrix Anal. Appl. 24 (2003) 1071–1109.

[15] Q.T. Jiang, P. Oswald, Triangular $\sqrt{3}$-subdivision schemes: The regular case, J. Comput. Appl. Math. 156 (2003) 47–75.

[16] Q.T. Jiang, P. Oswald, S.D. Riemenschneider, $\sqrt{3}$-subdivision schemes: Maximal sum rules orders, Constr. Approx. 19 (2003) 437–463.

[17] L. Kobbelt, $\sqrt{3}$-subdivision, in: SIGGRAPH Computer Graphics Proceedings, 2000, pp. 103–112.

[18] U. Labsik, G. Greiner, Interpolatory $\sqrt{3}$-subdivision, Comput. Graphics Forum 19 (2000) 131–138.

[19] G.Q. Li, W.Y. Ma, H.J. Bao, $\sqrt{2}$ subdivision for quadrilateral meshes, Vis. Comput. 20 (2004) 180–189.

[20] C. Loop, Smooth subdivision surfaces based on triangles, Master's thesis, University of Utah, Department of Mathematics, Salt Lake City, 1987.

[21] A. Lundmark, N. Wadströmer, H. Li, Hierarchical subsample giving fractal region, IEEE Trans. Image Process. 10 (2001) 167–173.

[22] P. Oswald, Designing composite triangular subdivision schemes, Comput. Aided Geom. Design 22 (2005) 659–679.

[23] P. Oswald, P. Schröder, Composite primal/dual $\sqrt{3}$-subdivision schemes, Comput. Aided Geom. Design 20 (2003) 135–164.

[24] V. Protasov, The geometric approach for computing the joint spectral radius, in: Proceedings of the 44th IEEE Conference on Decision and Control, and the European Control Conference 2005, Spain, December 12–15, 2005.

[25] H. Prautzsch, Analysis of $C^k$-subdivision surfaces at extraordinary points, preprint 04/98, Fakultät für Informatik, Universität Karlsuhe, Germany, 1998 (available at http://i33www.ira.uka.de).

[26] U. Reif, A unified approach to subdivision algorithms near extraordinary vertices, Comput. Aided Geom. Design 21 (1995) 153–174.

[27] K. Sahr, D. White, Discrete global grid system, in: Proc. 30th Symposium on Interface Computing Science and Statistics, 1998, pp. 269–278.

[28] M. Stamminger, G. Drettakis, Interactive sampling and rending for complex and procedural geometry, in: Proceedings of the Eurographics Workshop on Rendering 01, 2001, pp. 151–162.

[29] L. Velho, Quasi 4-8 subdivision, Comput. Aided Geom. Design 18 (2001) 345–357.

[30] L. Velho, D. Zorin, 4-8 subdivision, Comput. Aided Geom. Design 18 (2001) 397–427.

[31] L. Villemoes, Wavelet analysis of refinement equations, SIAM J. Math. Anal. 25 (1994) 1433–1460.

[32] A.B. Watson, A. Ahumada Jr., A hexagonal orthogonal-oriented pyramid as a model of image presentation in visual cortex, IEEE Trans. Biomed. Eng. 36 (1989) 97–106.

[33] D.X. Zhou, Norms concerning subdivision sequences and their applications in wavelets, Appl. Comput. Harmon. Anal. 11 (2001) 329–346.